PCCP

Accepted Manuscript

This is an *Accepted Manuscript*, which has been through the Royal Society of Chemistry peer review process and has been accepted for publication.

Accepted Manuscripts are published online shortly after acceptance, before technical editing, formatting and proof reading. Using this free service, authors can make their results available to the community, in citable form, before we publish the edited article. We will replace this *Accepted Manuscript* with the edited and formatted *Advance Article* as soon as it is available.

You can find more information about *Accepted Manuscripts* in the **Information for Authors**.

Please note that technical editing may introduce minor changes to the text and/or graphics, which may alter content. The journal's standard **Terms & Conditions** and the **Ethical guidelines** still apply. In no event shall the Royal Society of Chemistry be held responsible for any errors or omissions in this *Accepted Manuscript* or any consequences arising from the use of any information it contains.

Physical Chemistry Chemical Physics

ARTICLE

Interaction of *para-tert*-butylcalix[6]arene molecules in Langmuir films with cadmium ions and effects on molecular conformation and surface potential[†]

Ellen C. Wrobel,[a] Poliana M. Santos,[b] Márcio Lazzarotto,[c] Osvaldo N. Oliveira Jr,[d] Thiers M. Uehara,[d] Paulo B. Miranda,[d] Luciano Caseli,[e] Jarem R. Garcia,[a] Sérgio R. Lázaro,[a] Alexandre Camilo Jr,[f] Karen Wohnrath*[a]

In this paper, we employ the surface-specific polarization-modulated infrared reflection absorption spectroscopy (PM-IRRAS) and sum-frequency generation (SFG) methods with surface pressure and surface potential isotherms to determine the organization of *p-tert*-butylcalix[6]arene molecules and their interaction with Cd^{2+} ions in Langmuir monolayers. The area per molecule was estimated as 135 $Å^2$, which corresponds to the *Calix6* axis perpendicular to the air-water interface with most OH groups parallel to the interface. This area is larger than predicted by molecular modeling with quantum chemical calculations with a PM3 Hamiltonian (109 $Å^2$), which is ascribed to the repulsion between *Calix6* molecules. The incorporation of Cd^{2+} ions in the subphase leads to drastic changes in the dipole moment contribution of the monolayer surface potential. Rather than increasing with incorporation of Cd^{2+} ions owing to a decrease in the negative double-layer potential, the measured surface potential decreased monotonically with increasing ion concentration. This unexpected result was ascribed to a strong interaction with Cd^{2+} ions that induced the calyx of the molecule to adopt a more open conformation at the air/water interface and affected the orientation of hydration water molecules, according to the SFG data. This finding allows us to understand the reason why the Gouy-Chapman model fails to explain surface potential results for subphases containing divalent or trivalent ions, and may be relevant for application of calixarenes in sensing.

1. Introduction

Calixarenes are macrocyclic oligomers derived from phenol-formaldehyde condensation,[1,2] whose size and type of hydrophobic cavity can be varied and functionalized at the lower or upper rim.[1-3] Due to their cone-like structure[1-3] and presence of phenol oxygen donor atoms,[1-4] calixarenes may be complexed with metal ions or incorporate charged and neutral molecules.[1-5] With such properties, calixarenes have been used in detecting metallic ions, such as alkaline[6-8] and alkaline earth[8-10] metals, cadmium,[10-12] copper[7,13,14] and for incorporating neutral molecules,[15-20] including dopamine,[15] volatile organic compounds[16] and aminoacids.[17] They have been also studied in biological membranes,[18-20] and in the formation of molecularly organized films using self-assembled monolayers[21-23] and Langmuir-Blodgett (LB)[6-13,15-20] techniques. These organized films have been applied in metal ion sensors, biosensors, immunosensors and for encapsulating nanoparticles.

The ability of calixarenes to form LB films allows investigating molecular-level interactions responsible for complexation with metal ions that tend to yield more uniform films.[10] Ye *et al.*[13] observed trimers of *p-tert*-butylthiacalix[4]arene and Cu^{2+} ions in Langmuir and LB films, where the area per molecule at the air/water interface increased due to electrostatic repulsion among Cu^{2+} ions bound to

the complex. Hg^{2+} ions coordinated with *p-tert*-butylthiacalix[4]arene through the bridging-sulfur atom and its phenolic oxygen atoms, and were not located inside the calixarene cavities.[24] The presence of Cu^{2+} ions in the subphase induced a shift to lower areas per molecule and a decrease in collapse pressure of tetraoxocalix[2]arene[2]triazine, with the corresponding LB films being used as voltammetric sensors to detect Cu^{2+} ions.[25] Dong *et al.*[11] produced a sensor to measure trace levels of Tl^+ and Cd^{2+} made with an LB film of *p-tert*-butylthiacalix[4]arene, where the use of differential pulse stripping voltammetry led to a detection limit for Cd^{2+} of 2.10^{-8} mol L^{-1}. Recognition of metal ions through calixarenes has been studied theoretically[26,27] and experimentally,[6-14,24,25] in many cases motivated by the concern with the environment as heavy metals accumulate in biological systems.[24,28-30]

In this study, we investigate Langmuir films of the calixarene derivative *p-tert*-butylcalix[6]arene (referred to as *Calix6*), which has been the subject of previous studies.[6,31,32] We address two important issues, namely the orientation of *Calix6* molecules at the air/water interface, and their interaction with Cd ions from the subphase. With a combination of surface-specific spectroscopic techniques, viz. polarization-modulated infrared reflection-absorption spectroscopy (PM-IRRAS) and sum-frequency generation (SFG), and theoretical modeling, we obtained

information on molecular rearrangements of the film-forming molecules due to the interaction with divalent or trivalent ions. The main purpose is to solve the long-standing problem associated with the failure of the Gouy-Chapman model[33-35] to account for the double-layer potential in monolayers spread on subphases containing such types of ions.

2. Experimental section

Calix6 has been synthesized and purified according to the procedure described in the literature.[1,2] $CdCl_2$ and $Cd(CH_3COO)_2$ were purchased from Aldrich Co. Chloroform used as spreading solvent and all other chemical reagents were of analytical grade purity and used as received. Milli-Q water with 18.2 MΩ.cm resistivity was used in all the experiments. The Langmuir films were formed by spreading a chloroform solution of *para-tert-*butylcalix[6]arene on an aqueous subphase using a KSV 5000 Langmuir trough (KSV Instruments, Ltd., Helsinki, Finland) with an area of 15x53 cm^2. Surface pressure–area (π–A) and surface potential-area (ΔV-A) isotherms were obtained after evaporation of chloroform for 15 min, with a barrier speed of 10 mm min^{-1} at room temperature of ~20 ºC. The phase transitions and the elasticity of the monolayers were determined from the compressional modulus (Equation 1), where A is the molecular area at pressure π.

$$C_S^{-1} = -A.\left(\frac{\partial \pi}{\partial A}\right)_T \qquad [1]$$

Brewster angle microscopy (BAM) measurements were performed with a Plus System from Nanofilm Technologies (NFT - Germany), equipped with a 30 mW laser emitting *p*-polarized light at 690 nm, mounted on the Nima Langmuir trough housed in a class 10,000 clean room. The monolayers were compressed at the rate of 15 cm^2 min^{-1}. The polarization-modulated infrared reflection absorption (PM-IRRAS) spectra of *Calix6* monolayers spread on pure water and on $Cd(CH_3COO)_2$ solutions (9.10^{-3} mol L^{-1}) were recorded at ~ 20 ºC, with a KSV PMI 550 instrument (KSV Instrument, Ltd., Helsinki, Finland). The IR beam reached the monolayer at a fixed incidence angle of 80° and the resolution of the spectra was 8 cm^{-1}. The spectral range of the device is 1000-3000 cm^{-1}, and for facilitating visualization the spectra were divided into two regions, viz. from 1000-1800 and from 2800-3000 cm^{-1}, for the analysis of the C-H, C=C and C-O regions. Further information concerning the PM-IRRAS technique can be found in refs.[36,37]

The sum frequency generation (SFG) spectra were taken with a commercial SFG spectrometer (EKSPLA, Lithuania). Briefly, an active-passive mode-locked Nd^{+3}:YAG laser generates 30 ps pulses at a wavelength of 1064 nm, with a repetition rate of 20 Hz. It pumps a Harmonic Generator Unit that produces the second and third harmonic (532 nm and 355 nm, respectively). Part of the visible beam (532 nm) is used to excite the sample, together with a tunable IR pulse (from 4000 to 1000 cm^{-1}, 3 cm^{-1} resolution) generated by an Optical Parametric Generator/Optical Parametric Amplifier (OPG/OPA) pumped at 355 nm, coupled to a Difference Frequency Generation stage (DFG) which is pumped by a portion of the laser fundamental (1064 nm). The visible and IR pulses overlap spatially and temporally at the interface, generating the SFG signal in the reflection geometry. The incidence angles of the IR, visible and SFG beam were, respectively, 55°, 61° and ~ 60°. The overlap spot area of the pump beams (visible and infrared) on the sample was approximately 1 mm^2, and the pulse energies were 600 μJ and 120 μJ for the visible and infrared beams, respectively. The polarization combinations used in all measurements were SSP and SPS (S or P– polarization for SFG, visible and infrared beams, respectively). A Langmuir trough, with area 5 x 19.5 cm^2, was adapted to the SFG spectrometer to enable *in situ* measurements. The monolayer was

characterized via SFG both in pure water and with 9.10^{-3} mol L^{-1} of $CdCl_2$ in the subphase. The barriers speed was 8 mm min^{-1} and were stopped when the surface pressure reached ~30 mN m^{-1}. The spectra were taken from 2750-3050 cm^{-1} with 3 cm^{-1} steps (average of 100 laser shots per data point).

Molecular modeling for the *Calix6* molecule was carried with quantum chemical calculations using the Mopac 2009 package,[38] with the structure in vacuum shown in Figure 1 being obtained with the PM3 Hamiltonian. Theoretical molecular areas were calculated from the circle area, A = πr^2, where A is the area and r is the circle radius.
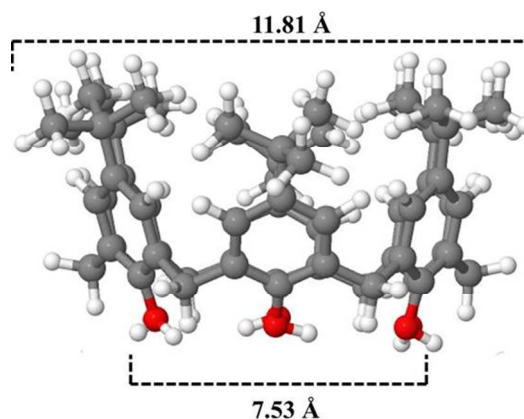
Fig. 1. *Calix6* molecular structures used for simulation in PM3 computational methodology. Oxygen atoms – red, Carbon atoms – gray, Hydrogen atoms – white.

3. Results and discussion

3.1. Langmuir films of *Calix6* on pure water

The surface pressure–area isotherm (π–A) for a Langmuir film of *Calix6* in Figure 2 features a collapse pressure of ~ 50 mN/m and area per molecule in the condensed phase, obtained by extrapolating the curve to zero pressure, of ca. 135 Å^2, which corresponds to the *Calix6* axis perpendicular to the air-water interface with most OH groups parallel to the interface. Since molecular orientation at the air/water interface cannot be obtained easily from the isotherms, we resorted to molecular modeling using Mopac package. The theoretical molecular area was calculated as 109.4 Å^2, corresponding to the area of the hydrophobic ring shown in Figure 1, whose diameter is 11.8 Å (circle radius = 5.9 Å). If the diameter of the hydrophilic ring in Figure 1 of 7.5 Å (circle radius = 3.8 Å) were used, the theoretical molecular area should be 54.4 Å^2. The *Calix6* molecule was assumed to adopt the cone conformation, considered the most stable for calixarene derivatives with six rings[31,39,40]. The difference to the experimentally observed value (135 Å^2) may be ascribed to two factors: i) the theoretical calculations were performed using zero Kelvin temperature, under vacuum, with no water molecules that could H-bond to *Calix6*. ii) repulsion between *Calix6* molecules, which is not taken into account in the theoretical modeling. A similar reasoning was adopted by Torrent-Burgués *et al*.[10] for the derivative *p-tert*-butylcalix[7]arene ethyl ester. A comparison with the literature is not straightforward because the packing of *Calix6* molecules appears to depend on the experimental conditions. For instance, Dei and coworkers[41] studied a similar derivative, the *p-tert*-butylcalix[8]arene, and observed that the area per molecule varied from 68 to 167 Å^2 when the spreading solvent was changed from chloroform to dichloromethane. In subsidiary experiments we found that the extrapolated area also depends on the concentration of *Calix6* in the spreading solution. Figure S1 in the

Supporting Information shows extrapolated areas ranging from ~190 to ~195 Å^2 when concentration was decreased to 0.1 and 0.3 mg mL^{-1}. These larger areas are consistent with other reports in the literature.[6,31,32] The inevitable conclusion is that *Calix6* may adopt more than one molecular arrangement at the air/water interface. For the remainder of this study, we fixed the concentration at 0.5 mg mL^{-1} for a stable arrangement, with reproducible isotherms and extrapolated area of 135 Å^2, was observed for this concentration and higher (we tested up to 1 mg mL^{-1}).
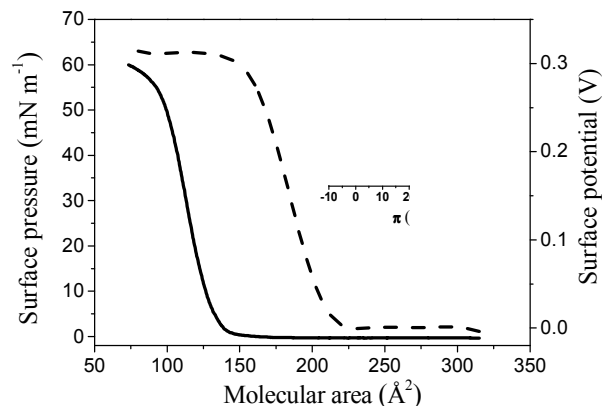
Fig. 2. Surface pressure-area (solid line) and Surface potential-area (dashed line) isotherms of *Calix6* (0.5 mg mL^{-1}) in CHCl$_3$ solution onto pure water. *Insert.* Compressibility modulus for *Calix6* monolayer.

The surface potential in Figure 2 was zero at large areas per molecule and increased sharply at a critical area near 220 Å^2 leveling off from 135 Å^2 and reaching 0.31 V (ΔV_{max}) for a condensed monolayer. The insert shows the compressibility modulus, calculated using Equation 1,[34,42] which provides information on the monolayer phase state. The C_S^{-1} maximum of ca. 197 mN m^{-1} is typical of a liquid-condensed phase,[34] and occurs at π= 27 mN m^{-1}. In subsidiary experiments, the compressibility was little affected by compression speed (in the range 5-15 mm min^{-1}) and time for solvent evaporation (15, 30 and 45 min).

Under high pressure, the *Calix6* molecules are believed to reorient according to a possible mechanism depicted in Figure 3, which consists in flipping the calyx upon compression. The probable repulsion and attraction interactions are also shown in Figure 3. Repulsion can explain the larger experimental value for the area per molecule (135 Å^2) compared to the theoretical area (109.4 Å^2). With closer proximity, repulsion between aromatic groups from *Calix6* and water takes place, while H-bonds are formed between the hydrophilic groups of *Calix6*. These two competing interactions lead to the tilting of the calyx.
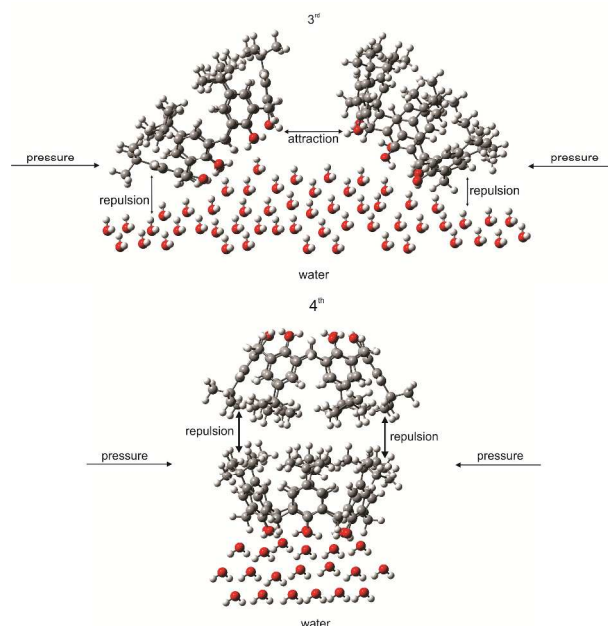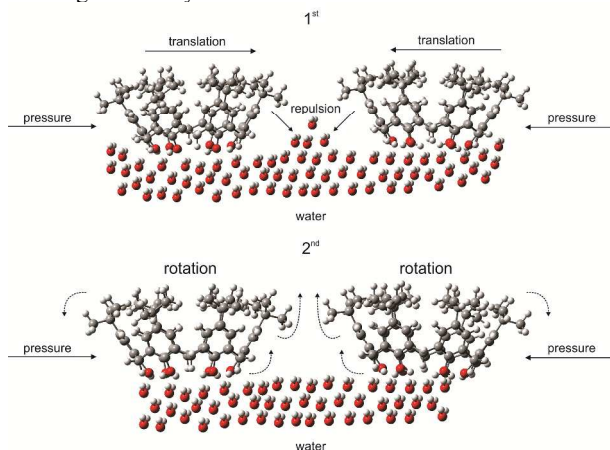
Fig. 3. Model for the arrangement of *Calix6* molecules under compression in a Langmuir film, where the 3rd step corresponds to the cone conformation assumed to be adopted in the condensed phase. The 4th step represents the collapse of the Langmuir film. The probable repulsion and attraction interactions are also depicted.

The PM-IRRAS spectra for Langmuir films of *Calix6* were obtained in the wavenumber range of 1000-3000 cm^{-1}, but only the regions where bands of interest appear are shown. For *Calix6* on the aqueous subphase, Figure 4a shows increasing intensity at higher pressures owing to the greater film density. The bands at 2860 and 2925 cm^{-1}, assigned to $\nu_s(CH_2)$ and $\nu_{as}(CH_2)$ stretching modes of the methylene bridges, are shifted by ~5 cm^{-1} to higher wavenumbers in the condensed monolayer (π = 25 mN m^{-1}). This shift could be related to disordering,[43] though it is within the experimental error of 8 cm^{-1}. The bands at 2893 and 2961 cm^{-1} are related to $\nu_s(CH_3)$ and $\nu_{as}(CH_3)$ stretching modes for the *tert*-butyl moieties. The C-H symmetric stretching in CH$_3$ is more pronounced at higher pressures, and there is a shift to lower wavenumbers at π = 10 mN m^{-1}.
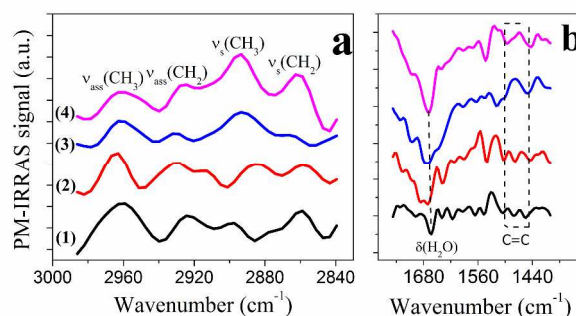
Fig. 4. PM-IRRAS spectra of *Calix6* spread on a pure water subphase at different surface pressures, where (1) 0 mN m^{-1}; (2) 10 mN m^{-1}; (3) 25 mN m^{-1} and (4) collapse: (a) in the alkyl chain vibration range (3000-2800 cm^{-1}); (b) in the range of bending mode δH_2O and C=C vibrations (1800-1400 cm^{-1}).

Figure 4b shows the PM-IRRAS spectra in the 1700-1400 cm^{-1} region, where the band at ~1670 cm^{-1} serves for monitoring the bending mode δH_2O[44] at the air-water interface. At π = 0 mN m^{-1}, this band appeared at 1
664 cm^{-1}, and at higher pressures the PM-IRRAS signal was intensified. Also, there was a shift to larger wavenumbers (1671 cm^{-1}

at π = 25 mN m^{-1}), which confirms its assignment to the liquid water absorption. This broad negative band is associated with an optical effect due to the strong dispersion of the refractive index of the liquid water subphase,[45,46] and may be explained by a thin layer of oriented water molecules beneath the surface layer.[47] Also in Figure 4b are shown the bands related to C=C vibrations (~1600-1400 cm^{-1}). The two upward-oriented bands between 1500 and 1450 cm^{-1} are broad at low pressures (0 and 10 mN m^{-1}) and overlap at higher pressures (25 mN m^{-1} and collapse), probably owing to aggregation of the molecules. The band at ~1425 cm^{-1} assigned to C−OH in-plane bending vibration only becomes well defined at high pressures (25 mN m^{-1} and collapse). This finding is consistent with the literature in that such band should only be well defined in Langmuir monolayers with accumulation of water at the interface.[48] From these PM-IRRAS data, one can infer that C-H and C=C vibrations are parallel to the interface, since upward-oriented bands indicate a parallel orientation to the surface plane.[46] These results are consistent with the theoretical model by which the *Calix6* adopts a flat-on arrangement on the interface.

3.2 Langmuir films of *Calix6* on subphases containing Cd^{2+} ions

There is evidence in the literature for the high selectivity of monolayers from calixarene derivatives toward Cs^{+}, Na^{+} and K^{+} ions,[6] with an increase in area per molecule that is proportional to the ionic radius of the metal. We could find no data for the interaction between *Calix6* monolayers and Cd^{2+} ions. The ability of complexation with Cd^{2+} ions (5.10^{-3} mol L^{-1}) was manifested by considerable changes in the isotherms in Figure 5 for *Calix6* monolayers with Cd^{2+} ions in the subphase. The most significant change was a shift toward larger areas per molecule in both surface pressure and surface potential isotherms. The area per molecule in the condensed phase increased from 135 Å^{2}, for pure water, to 160 Å^{2} for the Cd^{2+} subphase. This can be attributed to the formation of the [*Calix6*-Cd^{2+}] complex, where the increase in area is due to electrostatic repulsion among bound Cd^{2+} ions, as was reported for another calixarene derivative and Cu^{2+} ions in the subphase.[13]
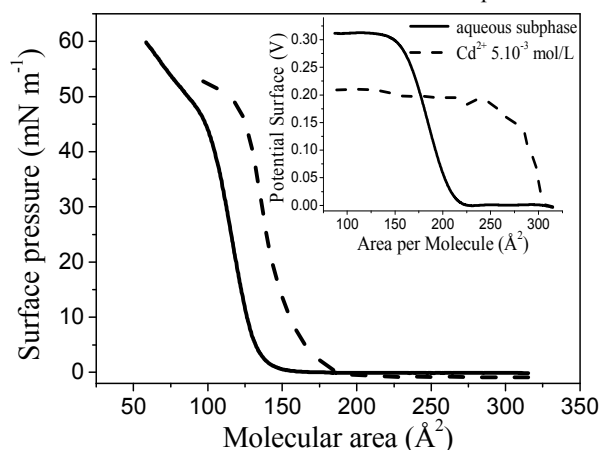
Fig. 5. Surface pressure-area isotherm for *Calix6* monolayers on water (solid line) or interacting with Cd^{2+} in the subphase, 5.10^{-3} mol L^{-1} (dashed line). *Insert.* Surface potential-area isotherm for *Calix6* monolayers on water (solid line) or interacting with Cd^{2+} in the subphase, 5.10^{-3} mol L^{-1} (dashed line).

The shift in area increased monotonically with the concentration of Cd^{2+} ions (Table 1), as shown in Figure S2 in the Supporting Information. The Cd^{2+} ion is unlikely to be inside the *Calix6* cavities; instead, the coordination with Cd^{2+} occurs through the phenolic oxygen atoms,[24] forming an exo-complex[5] at the air/water interface, which is confirmed with SFG experiments to be described later on. The monolayer compressibility decreased with

incorporation of Cd^{2+} ions to the subphase, as indicated in the C$_S^{-1}$ values in Table 1 obtained at π = 27 mN m^{-1}, where the *Calix6* monolayer showed decreased packing density.

Table 1. Mean molecular area (MMA), collapse pressure (π_{col}), compression modulus at π = 27 mN m^{-1} (C$_S^{-1}$) and surface potential maximum (ΔV_{max}) in Langmuir films of neat *Calix6* and with interaction with Cd^{2+} ions in the concentration range from 5.10^{-6} to 5.10^{-3} mol L^{-1}.

[Cd^{2+}] (mol L^{-1})	MMA (Å^2)	π_{col} (mN m^{-1})	ΔV_{max} (V)	C$_S^{-1}$ (mN m^{-1})
0	135	55	0.31	197
5.10^{-6}	144	51	0.30	147
1.10^{-5}	146	52	0.29	108
5.10^{-5}	148	55	0.26	160
1.10^{-4}	151	55	0.25	177
5.10^{-4}	155	51	0.24	135
1.10^{-3}	162	52	0.23	109
5.10^{-3}	163	51	0.21	163

The surface potential for *Calix6* in the insert of Figure 5 is lower for the condensed monolayer with the Cd^{2+}-containing subphase (5.10^{-3} mol L^{-1}). This is surprising because the incorporation of ions should decrease the negative contribution from the double-layer, thus causing the surface potential to increase. In order to understand this behavior, we recall that the measured surface potential can be related to the following contributions, according to the Demchak-Fort model in Equation 2.

$$\Delta V = \frac{1}{A\varepsilon_0}\left[\frac{\mu_1}{\varepsilon_1} + \frac{\mu_2}{\varepsilon_2} + \frac{\mu_3}{\varepsilon_3}\right] + \Psi \qquad [2]$$

where ΔV is the surface potential, ε_0 is vacuum permittivity and A is the area per molecule, μ_1 is the contribution from the reoriented water molecules, μ_2 is the dipole moment from the headgroups, μ_3 is the dipole moment from the tails, ε_i are the dielectric constants for each region of the interface, and ψ is the double-layer potential. The latter may be estimated using the Gouy-Chapman model[33,34] in Equation 3, where k is Boltzmann constant, T is the absolute temperature, e is the electronic charge, α is the degree of dissociation that depends on the subphase pH, and c is the ionic concentration of the subphase.[34]

$$\Psi = \frac{2kT}{e}\sinh^{-1}\left[\frac{e.\alpha}{A\left(5.88\times10^{-7}c.\varepsilon.T\right)^{\frac{1}{2}}}\right] \qquad [3]$$

According to Equations 2 and 3, if the dipole moment contributions were not changed (since only the subphase was altered), the surface potential was expected to increase with incorporation of Cd^{2+} ions, since the (negative) double-layer potential would be reduced. However, the data in Figure S3 in the Supporting Information show clearly that the surface potential decreased monotonically with an increasing concentration of Cd^{2+} ions (Table 1). This means that the positive dipolar component (μ_2 and μ_3) in the surface potential was decreased by addition of Cd^{2+} ions and that this reduction increased significantly (in magnitude) with Cd^{2+} concentration. Such reduction in dipolar moment can be explained by the changes caused by interaction between *Calix6* and Cd^{2+} ions observed in the spectroscopic measurements (see below).

That is to say, the reduction in the positive dipolar contribution surpasses the expected increase in surface potential caused by ion adsorption. In subsidiary experiments we noted that the surface potential indeed increased when monovalent ions, from NaCl, were added to the subphase, but it decreased for Cr^{3+} ions as it occurs for Cd^{2+} ions, as shown in Figure S4 and S5 in the Supporting Information.

Taken together, these results help resolve a long-standing problem associated with the interpretation of the double-layer contribution to the surface potential in Langmuir monolayers. The simple Gouy-Chapman (GC) theory can account for the experimental results of fatty acid monolayers on subphases containing monovalent salts, provided that the pH at the interface is calculated using the Henderson-Hasselbalch equation.[33] However, for divalent ion-containing subphases the GC theory is not able to explain the data, either because the assumptions on which it is based are no longer valid or because the divalent ions affect the dipole moment contribution to the monolayer surface potential. Here, we unequivocally showed that for the *Calix6* monolayer the incorporation of Cd (or Cr) ions leads to drastic changes in the dipole moment contribution. These changes are ascribed to a strong interaction with Cd ions that induced the calyx of the molecule to change conformation at the air/water interface and affected the orientation of hydration water molecules, according to data from the surface-specific spectroscopic techniques PM-IRRAS and SFG, as will be commented upon.

Significant differences are noted in the PM-IRRAS spectra for Langmuir films of *Calix6* on aqueous and Cd^{2+} subphases at $\pi = 25$ mN m^{-1} in Figure 6a. The band at 2930 cm^{-1}, attributed to C−H antisymmetric stretching in CH_2, is shifted to higher wavenumbers (2932 cm^{-1}) with increased intensity when Cd^{2+} ions are present. On the other hand, the weak band at 2865 cm^{-1}, attributed to $vs(CH_2)$, disappears with incorporation of Cd^{2+}. These results indicate that complexation affects the orientation of methylene bridges. The CH_3 stretching bands of *tert*-butyl moieties are also sensitive to complexation, whereas the band at 2961 cm^{-1}, attributed to C−H antisymmetric stretching in CH_3, practically disappears and a new band appears at 2974 cm^{-1}. The C−H symmetric stretching in CH_3 at 2893 cm^{-1} is shifted to lower wavenumbers to 2878 cm^{-1}. Consistent with Korchowiec et al.,[8] we conclude that the calixarene *tert*-butyl moieties are sensitive to divalent cations, and hence complexation modifies intermolecular interactions among groups in the upper rim. In the 1600-1800 cm^{-1} region, Figure 6b shows a negative band for the *Calix6* monolayer at ~ 1670 cm^{-1}, due to the $\delta(H_2O)$ bending mode of the liquid water subphase. New bands appear at 1640 and 1690 cm^{-1}, i.e. the Langmuir film of [*Calix6*-Cd^{2+}] affects organization of water molecules. The band at ~ 1730 cm^{-1} is assigned to $v(C=O)$ of the acetate ion of cadmium salt in the subphase, i.e., the oriented counterion in the electric double-layer. Figure 6b shows that the band assigned to C=C vibrations is upward-oriented at ~1478 cm^{-1} in absence of Cd^{2+} ions, being shifted slightly to higher energies when Cd^{2+} ions are present.

Coordination with Cd^{2+} ions occurs at phenolic oxygen atoms, as indicated in the PM-IRRAS spectra in Figure S6 in the Supporting Information. The band at ~1425 cm^{-1}, assigned to C-OH in-plane bending vibration, is less defined at high pressures, when the Cd^{2+} ions are present. This is due to Cd-O bonds, confirming the exo-complex formation at the air-water interface, which is corroborated by SFG results discussed below.
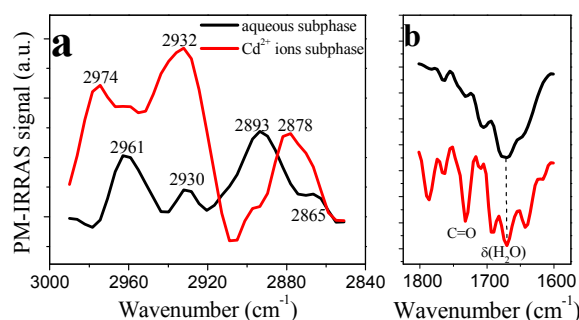
Fig. 6. PM-IRRAS spectra of *Calix6* spread on a pure water and Cd^{2+} (9.10^{-3} mol L^{-1}) subphase at $\pi = 25$ mN m^{-1}: (a) in the alkyl chain vibration range (3000-2800 cm^{-1}); (b) in the range of bending mode δH_2O (1800-1600 cm^{-1}).

The SFG spectra for Langmuir films of *Calix6* spread on water and on a subphase containing $CdCl_2$ (9.10^{-3} mol L^{-1}) are shown in Figure 7 for the polarization combinations SSP and SPS. For an isotropic surface, the SSP polarization (IR is P-polarized) is more sensitive to vibrations with the IR transition dipole closer to the surface normal, while the SPS polarization (S-polarized IR) is enhanced for groups with the IR transition dipole with a large tilt from the surface normal (but not parallel to the surface, since in this case the SFG signal should vanish in all polarizations). It should also be stressed that *Calix6* dimers in the multilayers should not contribute to the SFG spectra, since they would have inversion symmetry and therefore a vanishing second-order nonlinear polarizability. The concentration of Cd^{2+} ions was chosen based on studies to detect Cd^{2+} ions in Langmuir films, since Torrent-Burgués et al.[10] observed the isotherms of *p-tert*-butylcalix[n]arene-ethyl ester (n=4 and 7) to be affected by Cd^{2+} ions at concentrations close to 1.10^{-2} mol L^{-1}.
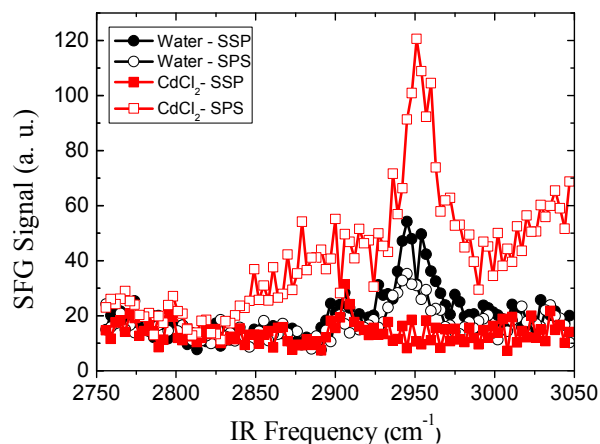
Fig. 7. SFG spectra of *Calix6* spread on a pure water and Cd^{2+} ions subphase (9.10^{-3} mol L^{-1}) at $\pi = 30$ mN m^{-1}.

The pronounced peak at ~2950 cm^{-1} and the weaker one near 2900 cm^{-1} in the SFG spectra of Figure 7 can be assigned to the CH_3 asymmetric and symmetric stretches of the *tert*-butyl groups, respectively.[49] The simple fact that there is SFG signal indicates that *Calix6* molecules in the monolayer lay on the water surface as monomers, with -OH groups pointing towards and hydrogen bonding to water. This is consistent with the structure proposed in the theoretical calculation, and with the inference from the PM-IRRAS spectra (Figure S6 in the Supporting Information) that the C-OH vibration band arises from Cd-O bonds. There is a clear

difference in Figure 7 for the intensity ratio of CH_3 asymmetric stretch (~2950 cm^{-1}) with SSP and SPS polarization combinations, which reflects the average orientation of CH_3 groups. On pure water, the intensity for SSP is slightly higher than for SPS, whereas on the subphase containing Cd^{2+} the SSP peak nearly vanishes while the SPS intensity has increased about four times. This is evidence for reorientation of methyl groups of calix[6]arene with the addition of Cd^{2+}. As the *tert*-butyl groups have their CH_3 groups with a 3-fold symmetry, most likely we are probing the contribution of the asymmetric stretch of each CH_3 group projected along the arene axis. Therefore, an increase in the SPS contribution for the asymmetric stretch indicates that the arene group is increasingly tilted away from the surface normal when Cd^{2+} ions are present in the subphase, while in pure water the arene group adopts a more upright orientation. This suggests that the monolayer is mostly comprised of *Calix6* monomers with their axes perpendicular to the surface, but their conformation is affected by the interaction with Cd^{2+} ions, with a "crown conformation" (arene groups are more upright) on pure water and an "open calyx conformation" induced by the interaction of Cd^{2+} ions with the -OH dipoles in the lower rim (see sketch in Figure 8). This interaction with the ion leads the *Calix6* to be more open, occupying a large molecular area, in agreement with the expansion of the isotherm in Figure 5. A similar conformational change in cavitands (vase to kite) induced by interaction with Zn^{2+} ions[50] or by pH[51] has been observed at the air-water interface. Furthermore, with incorporation of Cd^{2+} ions in the subphase, aggregation starts at a much lower surface pressure ($\pi = 5$ mN m^{-1}), as indicated in the BAM images in Figure S7 in the Supporting Information. Therefore, the complex [Cd^{2+}-*Calix6*] facilitates aggregation, perhaps with Cd^{2+} ions mediating dimer[39] formation.
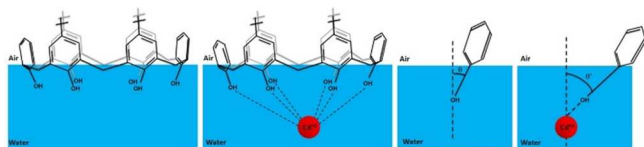
Fig. 8. Structure of *Calix6* on (a) aqueous and (b) Cd^{2+} ions subphase. Angle θ between arene group of *Calix6* on water subphase (c) is smaller than θ' for the *Calix6* on Cd^{2+} ions subphase (d).

4. Conclusions

With a combination of surface pressure isotherms and surface-specific vibrational spectroscopic methods, we could determine the orientation of *Calix6* molecules in Langmuir monolayers. These molecules are believed to adopt a flat-on arrangement on the interface with their O-H groups pointing toward the aqueous subphase, in contrast to a few reports in the literature.[6,31,32] The experimentally observed area per molecule for a condensed monolayer was larger than predicted by theoretical modeling with quantum chemical calculations with a PM3 Hamiltonian, owing to repulsion between *Calix6* molecules, which is not considered in the theoretical modeling. The *Calix6* molecules are rearranged upon compression owing to the flipping of the calyx induced by a competition between repulsion forces, involving aromatic groups from *Calix6* and water, and H-bonds among hydrophilic groups of *Calix6*.

The incorporation of Cd^{2+} ions induced a large expansion in the surface pressure and surface potential isotherms owing to the electrostatic repulsion among bound Cd^{2+} ions in [*Calix6*-Cd^{2+}] complex. From the PM-IRRAS and SFG results, we inferred that the Cd^{2+} ion was coordinated through the phenolic oxygen atoms to form an exo-complex, with an "open calyx conformation" resulting from the interaction of Cd^{2+} ions with the -OH dipoles in the lower rim. Such open conformation led to the larger area per molecule. With this drastic change in conformation, one should expect a large change in the molecular dipole moment caused by Cd^{2+} ions. Indeed, the surface potential for the *Calix6* monolayer on a Cd-containing subphase was lower than for the monolayer on pure water, in contrast to the expected increase owing to the lowering of the negative contribution of the double-layer.

The main contributions in this paper can be summarized as follows. The molecular conformation of *Calix6* in Langmuir films, including the rearrangement induced by compression, could be determined by combining surface pressure isotherms, surface-specific spectroscopic measurements and theoretical modeling. Furthermore, we showed why the Gouy-Chapman model fails to explain the surface potential data when a divalent ion is present. In contrast to what was widely believed in the literature, the failure is not associated with simplifications in premises adopted for developing the Gouy-Chapman theory, but is rather due to changes in the dipolar contribution to the surface potential. Significantly, the precise information on the effects from Cd^{2+} ions may be relevant for application of calixarenes in sensing.

Notes and references

^{a}*Departamento de Química, Universidade Estadual de Ponta Grossa (UEPG), Ponta Grossa, Paraná (PR) 84030-900, Brazil.*
^{b} *Universidade Tecnológica Federal do Paraná, 81280340 - Curitiba, PR - Brazil.*
^{c}*Instituto de Química, Departamento de Química Orgânica, Universidade Federal do Rio Grande do Sul, Porto Alegre, Rio Grande do Sul (RS) 91501-970, Brazil.*
^{d}*Instituto de Física de São Carlos, Universidade de São Paulo, CP 369, São Carlos, São Paulo (SP) 13560-970, Brazil.*
^{e}*Instituto de Ciências Ambientais, Químicas e Farmacêuticas, Universidade Federal de São Paulo, Diadema, São Paulo (SP) 09972-970, Brazil.*
^{f}*Departamento de Física, Universidade Estadual de Ponta Grossa (UEPG), Ponta Grossa, Paraná (PR) 84030-900, Brazil.*
*e-mail address: karen.woh@gmail.com

† Electronic supplementary information (ESI) available: π-A isotherms of *Calix6* monolayers at different concentrations; Surface pressure-area and Surface potential area isotherms of *Calix6* on Cd^{2+}, Na^+ and Cr^{3+} ions subphases, at different concentrations; PM-IRRAS spectra of *Calix6* on aqueous and Cd^{2+} ion subphases (1800-1600 cm^{-1}); Brewster Angle Microscopy images for *Calix6* in aqueous and Cd^{2+} ions subphases under different surface pressures. See DOI:.

1   C.D. Gutsche, in *Calixarenes: an introduction*; ed. Thomas Graham House, Royal Society of Chemistry, Cambridge, 2nd ed., 2008, pp 27-88.

2   C. D. Gutsche, B. Dhawan, K. H. No and R. Muthukrishnan. Calixarenes. *J. Am. Chem. Soc.,* 1981, **103**, 3782-3792.

3   C. D. Gutsche, in Calixarenes Revisited; The Royal Society of Chemistry, Cambridge, 1998, pp 10-62.

4   D. Mendoza-Espinosa, B. A. Martinez-Ortega, M. Quiroz-

Guzman, J. A. Golen, A. L. Rheingold and T. A. *J. Organomet. Chem.* 2009, **694**, 1509–1523.

5   A. J. Petrella and C. L. Raston. *J. Organomet. Chem.* 2004, **689**, 4125–4136.

6   L. Dei, A. Casnati, P. LoNostro and P. Baglioni. *Langmuir.* 1995, **11**, 1268-1272.

7   F. L. Supian, T. H. Richardson, M. Deasy, F. Kelleher, J. P. Ward and V. McKee. *Langmuir.* 2010, **26**, 10906–10912.

8   B. Korchowiec, M. Orlof, G. Sautrey, A. B. Salem, J. Korchowiec, J. Regnouf-de-Vains and E. Rogalska. *J. Phys. Chem. B.* 2010, **114**, 10427–10435.

9   B. Lonetti, E. Fratini, A. Casnati, P. Baglioni. *Colloids Surf., A.* 2004, **248**, 135–143.

10 J. Torrent-Burgués, F. Vocanson, J. J. Pérez-González, A. Errachid. *Colloids Surf., A.* 2012, **401**, 137–147.

11 H. Dong, L. Zheng, L. Lin and B. Ye. *Sens. Actuators, B.* 2006, **115**, 303–308.

12 A. V. Nabok, T. Richardson, F. Davis and C. J. M. Stirling. *Langmuir.* 1997, **13**, 3198-3201.

13 Z. Ye, S. Pang, W. He, X. Shi, Z. Guo and L. Zhu. *Spectrochim. Acta, Part A.* 2001, **57**, 1443–1447.

14 A. Castillo, J. L. Martínez, P. R. Martínez-Alanis and I. Castillo. *Inorg. Chim. Acta.* 2010, **363**, 1204-1211.

15 P. Vitovic, D. P. Nikolelis and T. Hianik. *Biochim. Biophys. Acta.* **2006**, 1758, 1852–1861.

16 R. Çapan, Z. Özbek, H. Göktas, S. Sen, F. G. Ince, M. E. Özel, G. A. Stanciu and F. Davis. *Sens. Actuators, B.* 2010, **148**, 358-365.

17 M. W. Sugden, T. H. Richardson, F. Davis, S. P. J. Higson, and C. F. J. Faul. *Colloids Surf., A.* 2008, **321**, 43–46.

18 P. Shahgaldian, M. A. Sciotti and U. Pieles. *Langmuir.* 2008, **24**, 8522-8526.

19 G. Sautrey, I. Clarot, E. Rogalska, and J. Regnouf-de-Vains. *New J. Chem.* 2012, **36**, 2060–2069.

20 B. Korchowiec, M. Gorczyca, A. B. Salem, J. Regnouf-de-Vains and E. Rogalska. *Colloids Surf., B.* 2013, **103**, 217–222.

21 B. Tieke, A. El-Hashani, A. Toutianoush and A. Fendt. *Thin Solid Films.* 2008, **516**, 8814-8820.

22 S. Gao, D. Yuan, J. Lü and R. Cao. *J. Colloid Interface Sci.* 2010, **341**, 320–325.

23 H. Chen, J. Lee, W. Jo, M. Jeong and K. Koh. *Microchim. Acta.* 2011, **172**, 171–176.

24 F. Wang, X. Wei, C. Wang, S. Zhang and B. Ye. *Talanta.* 2010, **80**, 1198–1204.

25 L. Zou, Y. Li, W. Zhao, S. Zhang, B. Ye. *J. Solid State Electrochem.* 2012, **16**, 505-511.

26 J. Liu, Q. Zheng, C. Chen and Z. Huang. *Tetrahedron.* 2007, **63**, 9939–9946.

27 A. S. de Araujo, O. E. Piro, E. E. Castellano and A. F. D. de Namor. *J. Phys. Chem. A.* 2008, **112**, 11885–11894.

28 K. C. Honeychurch, J. P. Hart, D. C. Cowell and D. W. M. Arrigan. *Sens. Actuators, B.* 2001, **77**, 642-652.

29 M. A. Qazi, I. Qureshi and S. Memon. *J. Mol. Struct.* 2010, **975**, 69–77.

30 L. Friberg. *Annu. Rev. Public Health.* 1983, **4**, 367-373.

31 P. LoNostro, A. Casnati, L. Bossoletti, L. Dei and P. Baglioni. *Colloids Surf., A.* 1996, **116**, 203-109.

32 B. Lonetti, P. LoNostro, B. Ninham and P. Baglioni. *Langmuir.* 2005, **21**, 2242-2249.

33 D. M. Taylor, O. N. Oliveira Jr and H. Morgan. *Chem. Phys. Lett.* 1989, **161**, 147-150.

34 J. T. Davies and E. K. Rideal, in *Interfacial Phenomena*; Academic Press, New York, 1963, pp 56-275.

35 A. W. Adamson, in *The Physical Chemistry of Surfaces*, ed John Wiley & Sons, Interscience, New York, 6th ed., 1990, pp 537-560.

36 R. Mendelsohn, G. Mao and C. R. Flach. *Biochim. Biophys. Acta.* 2010, **1798**, 788–800.

37 L. Caseli and J. R. Siqueira Jr. *Langmuir.* 2012, **28**, 5398−5403.

38 J. J. P. Stewart. MOPAC2009, Stewart Computational Chemistry, Colorado Springs, CO, USA, 2008.

39 G. D. Andreetti, G. Calestani, F. Ugozzoli, A. Arduini, E. Ghidini, A. Pochini and R. Ungaro. *J. Inclusion Phenom.*, **1987**, 5, 123-126.

40 A. N. Novikov, V. A. Bacherikov and A. I. Gren. *Russ. J. Gen. Chem.* 2002, **72**, 1396-1400.

41 L. Dei, P. LoNostro, G. Capuzzi and P. Baglioni. *Langmuir.* 1998, **14**, 4143-4147.

42 M. C. Petty, in *Langmuir-Blodgett Films: An introduction*, Cambridge University Press, Cambridge, 1996.

43 K. Czapla, B. Korchowiec and E. Rogalska. *Langmuir.* 2010, **26**, 3485–3492.

44 J. Saccani, S. Castano, F. Beaurain, M. Laguerre and B. Desbat. *Langmuir.* 2004, **20**, 9190-9197.

45 M. Dyck, A. Kerth, A. Blume and M. Lösche. *J. Phys. Chem. B.* 2006, **110**, 22152-22159.

46 W. Ulrich and H. Vogel. *Biophys. J.* 1999, **76**, 1639–1647.

47 D. Blaudez, J. Turlet, J. Dufourcq, D. Bard, T. Buffeteau and B. Desbat. *J. Chem. Soc., Faraday Trans.* 1996, **92**, 525–530.

48 T. E. Goto and L. Caseli. *Langmuir.* 2013, **29**, 9063−9071.

49 Ö. Dereli, Y. Erdogdu, M. T. Gulluoglu, E. Türkkan and A. Özmen. *J. Mol. Struct.* 2012, **1012**, 168–176.

50 M. Frei, F. Marotti and F. Diederich. *Chem. Commun.,* 2004, 1362-1363.

51 P. Pagliusi, F. Lagugné-Labarthet, D. K. Shenoy, E. Dalcanale, Y. R. Shen. *J. Am. Chem. Soc.*, 2006, **128**, 12610-12611.